

The Life Cycle of Stratospheric Aerosol Particles



Patrick Hamill,* Eric J. Jensen,+ P. B. Russell,+ and Jill J. Bauman#

ABSTRACT

This paper describes the life cycle of the background (nonvolcanic) stratospheric sulfate aerosol. The authors assume the particles are formed by homogeneous nucleation near the tropical tropopause and are carried aloft into the stratosphere. The particles remain in the Tropics for most of their life, and during this period of time a size distribution is developed by a combination of coagulation, growth by heteromolecular condensation, and mixing with air parcels containing preexisting sulfate particles. The aerosol eventually migrates to higher latitudes and descends across isentropic surfaces to the lower stratosphere. The aerosol is removed from the stratosphere primarily at mid- and high latitudes through various processes, mainly by isentropic transport across the tropopause from the stratosphere into the troposphere.

1. Introduction

During the past 20 years our knowledge of the characteristics of the stratospheric aerosol has increased dramatically. The first quantitative studies of the stratospheric aerosol were made during the 1960s by C. Junge (Junge et al. 1961), who noted that as balloon-borne instruments rose into the stratosphere, they registered an increase in the number of large particles (average radius $> 0.15 \mu\text{m}$). About 10 years later J. Rosen showed that the boiling point of the particles was consistent with a sulfuric acid solution with a composition of about 75% H_2SO_4 and 25% H_2O (Rosen 1971). Observations of the aerosol layer by in situ observations from aircraft and balloons (Rosen 1964), as well as by remote sensing by lidar (Fiocco and Grams 1964; McCormick et al. 1984) and satellites (McCormick

et al. 1979), allowed researchers to determine the global characteristics of this aerosol. It was found that the aerosol layer extends from somewhat above the tropopause to about 30-km altitude, that the extinction ratio (ratio of aerosol extinction to molecular extinction) at a wavelength of $1.02 \mu\text{m}$ is typically in the range of 2 to 6, that the aerosol undergoes seasonal variations, and that it is highly influenced by large volcanic eruptions.

Modeling studies paralleled the observational programs. Hamill et al. (1977b) described the basic microphysical processes affecting the stratospheric aerosol particles, and Toon et al. (1979) and Turco et al. (1979) successfully used a one-dimensional microphysical model to describe most of the properties of the layer. More recently, Tie et al. (1994) applied model studies to the aerosol produced by the eruption of El Chichón, and Zhao et al. (1995b) used a model to study the formation of the stratospheric volcanic clouds due to Mt. Pinatubo. Models of the stratospheric sulfate aerosol have also been developed for special studies, such as for determining the effects of supersonic transports (Pitari et al. 1993).

It was observed that after the eruptions of El Chichón, Pinatubo, and other energetic volcanic explosions the aerosol is highly enhanced as a result of injections of water and sulfur dioxide into the stratosphere. It is believed that the sulfur diox-

*Department of Physics, San Jose State University, San Jose, California.

+NASA/Ames Research Center, Moffett Field, California.

#State University of New York at Stony Brook, Stony Brook, New York.

In final form 6 January 1997.

Corresponding author address: Dr. Patrick Hamill, Department of Physics, San Jose State University, College of Science, 1 Washington Square, San Jose, CA 95192-0106.

E-mail: hamill@sky.arc.nasa.gov

©1997 American Meteorological Society

ide is transformed into sulfuric acid with an e -folding time of about 1 month (Young et al. 1994; Read et al. 1993) and that, subsequently, sulfuric acid and water combine to form new sulfuric acid solution droplets by the process of heteromolecular homogeneous nucleation. During the past 15 years, satellite observations of the stratospheric aerosol have shown significant increases in the mass of the layer following volcanic eruptions; these are followed by a gradual decrease in mass. Although it is difficult to ascertain exactly when the aerosol reaches a steady-state condition, it is believed that previous to the eruptions of Fuego, El Chichón, and perhaps Pinatubo the observed aerosol was very close to the background level. Thomason et al. (1997) argue that an equilibrium or background aerosol was not achieved and the tropical stratosphere still contained volcanically derived aerosols up to the time of the eruption of Mt. Pinatubo. Some researchers have postulated that the emissions from small volcanic eruptions may contribute to the aerosol during periods between large volcanic eruptions (Hitchman et al. 1994). Recent observations and analyses presented by Brock et al. (1995) strongly suggest a tropical source for the nonvolcanic stratospheric sulfate particles. In this

paper we accept the existence of a background nonvolcanic aerosol and we study the microphysical processes that maintain it. Our intention is to sketch a picture of the life cycle of the stratospheric aerosol. This picture is based on a combination of observations and microphysical calculations, but its validity will ultimately depend on agreement with detailed measurements. In particular, we enquire how the sulfuric acid particles are formed, how a size distribution develops, and how the particles are eventually removed from the stratosphere. With the exception of the formation mechanisms considered in section 2, most of the discussion in this paper is also applicable to aerosols generated by volcanic eruptions that inject sulfur-bearing gases into the tropical stratosphere.

Figure 1 is a cartoon illustrating the basic premise of this paper. Note that there are three main processes affecting the life cycle of an aerosol. The first is the formation of the aerosol particles by nucleation in a rising tropical air mass. Nucleation is followed by coagulation, growth by condensation, and mixing with air containing aged aerosol particles, generating an aerosol with the observed size distribution. During this time, the aerosol circles the earth continuously, forming part of the “tropical stratospheric reservoir” first described by Trepte and Hitchman (1992) and also discussed by Grant et al. (1996). After volcanic eruptions, there appears to be some transport of stratospheric material to midlatitudes at altitudes near the tropopause; therefore, it must be assumed that near the tropopause there is a possibility for matter to easily be transported out of the tropical region. However, most of the material is trapped in the reservoir, spreading poleward during the westerly shear phase of the quasibiennial oscillation and being compacted nearer the equator during the easterly phase. The aerosol is eventually transported to midlatitudes, crossing the boundaries of the “leaky tropical pipe” (Plumb 1996) in the 15°–30° latitude range. Trepte and Hitchman

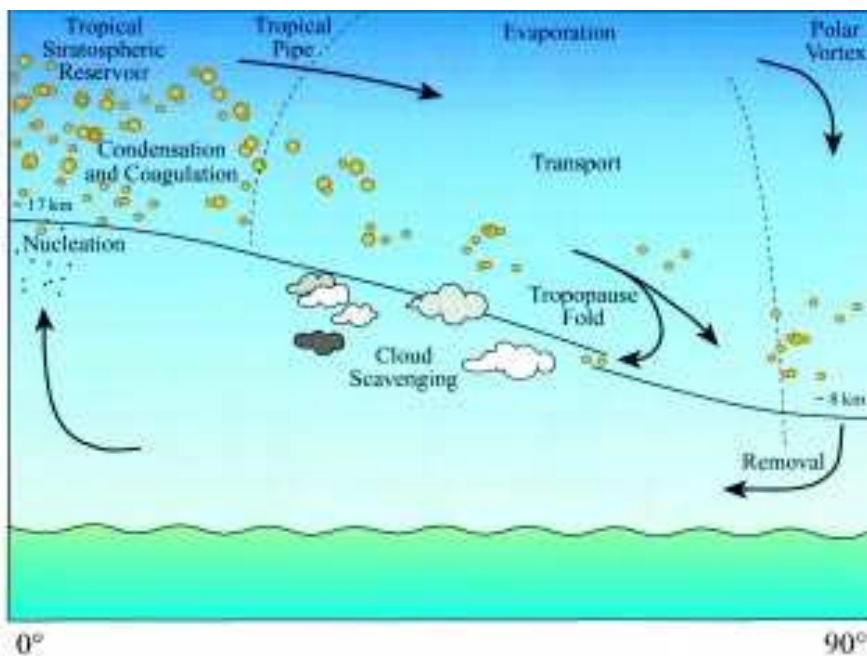


FIG. 1. The life cycle of a stratospheric aerosol. The aerosol particles are formed by homogeneous nucleation in rising tropical air and grow by condensation and coagulation as they are carried aloft. They eventually move to midlatitudes where they may be removed by mixing across the tropopause. Some will be incorporated into the polar vortex and carried down into the troposphere by descending air.

(1992) show that within a few kilometers of the tropopause, aerosol particles are readily transported poleward, but the transport of particles in the 21–28-km altitude range is inhibited and controlled by the phase of the quasi-biennial oscillation. When the aerosol reaches midlatitudes, it continues to circle the earth but slowly descends across isentropic surfaces to the region called the “lowermost stratosphere” by Holton et al. (1995) and the “middleworld” by Hoskins (1991). When the aerosol is in the mid- and high latitudes, there may be a continuous monotonic growth of the particles due to the absorption of sulfuric acid vapor generated from the carbonyl sulfide (OCS) and SO_2 that diffuses into the stratosphere (Turco et al. 1979). It might be mentioned, however, that recent studies cast doubt on the role of OCS in contributing to the sulfate layer (Chin and Davis 1995). Thus it is possible that most or all of the growth has taken place in the tropical reservoir. At any rate, a very slow change in aerosol size due to condensation will be masked by the larger-size changes related to the absorption and evaporation of water due to variations in the environmental temperature. This results in variations in the extinction (and optical depth) of the aerosol layer that are consistent with satellite observations, including the latitudinal and seasonal variations in optical depth as evidenced by measurements obtained with the Stratospheric Aerosol and Gas Experiment (SAGE) satellite system. Finally, the aerosol will be removed from the stratosphere. Particles contained in air masses that descend nonisentropically at midlatitudes can be carried back toward the Tropics and transported out of the stratosphere, most probably in a tropopause fold. This is probably the principal loss mechanism for stratospheric aerosols, although other isentropic and diabatic exchange processes, as discussed below, may be significant. Some particles will be lost from the stratosphere by being entrained into the polar winter vortex and removed as the air in the vortex descends into the troposphere. An aerosol particle that has survived for a very long time in the stratosphere may grow large enough to sediment to the tropopause. Some aerosol particles will rise to higher altitudes where the temperature is warmer and will evaporate. Scavenging by clouds piercing the tropopause is a possible but little understood removal mechanism.

We describe the initial formation of the aerosol in the Tropics by nucleation and coagulation in sec-

tion 2. In section 3 we discuss the growth of the aerosol particles by heteromolecular condensation and we also describe the seasonal growth and evaporation of midlatitude aerosols. Removal processes are outlined in section 4. We do not consider transport processes in any detail but, following the scheme outlined by Holton et al. (1995), we assume that air rises in the Tropics, moves out of the Tropics, and descends into the extratropical lower stratosphere (the lowermost stratosphere). This is, of course, essentially the Brewer–Dobson circulation described by Brewer (1949) and Dobson (1956). Once the air has descended into this region of the stratosphere, it can be transported isentropically into the troposphere. Aerosol particles are, of course, carried along with these air masses. As soon as the particles reach the troposphere they are lost, primarily by scavenging in clouds. It should be pointed out, however, that diabatic processes also occur in the lowest levels of the stratosphere.

We assume that the background stratospheric aerosol particles are liquid-phase sulfuric acid solutions. In situ observations with aircraft and balloons indicate that the unperturbed background sulfate aerosol consists of particles having a log-normal size distribution peaked at about $0.07\text{-}\mu\text{m}$ radius and having a number density of about 10 cm^{-3} (Pinnick et al. 1976). We do not consider in this paper the ice or nitric acid solution particles that form in the polar winter stratospheres (McCormick et al. 1982).

2. Nucleation and coagulation of new particles

In this section we first describe the nucleation of sulfuric acid particles in an ascending air mass in the Tropics. It was noted by Goodman et al. (1982), from measurements made with the National Aeronautics and Space Administration (NASA) U2 aircraft flying out of Panama, that convective activity at the intertropical convergence zone may be a source mechanism for stratospheric aerosols. This conclusion was based on the fact that size distributions near the tropopause suggested “young” aerosols, compared to size distributions at higher altitudes. Yue and Deepak (1984) noted that SAGE aerosol extinctions were consistent with the upper troposphere in the Tropics being a source of condensation nuclei in the stratosphere. Recent mea-

measurements and theoretical studies by Brock et al. (1995) show that the tropical tropopause is a region where new particle formation takes place. This suggests that the background sulfate aerosol is formed in the Tropics and spends its lifetime in the Tropics or migrating to a region where it will be removed from the stratosphere.

a. Nucleation

Consider an air parcel at an altitude of about 15 km and located near the equator. Suppose this air parcel is ascending. The average value of vertical air velocities in the Tropics at 70 mb is $2 \times 10^{-4} \text{ m s}^{-1}$ (Rosenlof 1995). One would expect the instantaneous vertical velocity of a particular air parcel to be much greater (or much less) than this value. Nevertheless, for our purposes the actual vertical velocity of an air parcel is not important as long as the air is ascending.

Air in the upper troposphere has been “processed” by clouds and is usually devoid of large aerosols. As Jensen et al. (1996) have shown, at the tropical tropopause there is frequent formation of subvisible cirrus clouds composed of ice crystals of about $10 \mu\text{m}$ in radius and with a number density of 0.1 cm^{-3} . Brock et al. (1995) and Clarke (1993) observed that particles are nucleating in this region. Here we show that in this region the nucleation rate is high; then we show that the newly formed particles can survive until carried aloft into the stratosphere, that is, we show that the newly nucleated sulfate particles will not be scavenged by ice crystals before reaching the stratosphere.

We have carried out a nucleation rate calculation using the temperature profile illustrated on the left-hand side of Fig. 2. This is the standard atmosphere cold tropical temperature profile (COESA 1967). We also used the standard atmosphere water vapor profile and used a sulfuric acid profile obtained from the NASA/Ames one-dimensional model. The estimated sulfuric acid concentrations ranged from $7.5 \times 10^4 \text{ molecules cm}^{-3}$ at 16 km to $3.9 \times 10^4 \text{ molecules cm}^{-3}$ at 18 km. The nucleation rates we obtained are presented in the right-hand panel of Fig. 2. These nucleation rates are quite large. For example, if the air parcel is rising at 1 m s^{-1} (which is probably an unrealistically large vertical velocity), it will require 1000 s to rise 1 km. At a nucleation rate of 300 s^{-1} , one would form over 10^5 new particles cm^{-3} . (This is more particles than our assumed number of sulfuric acid mol-

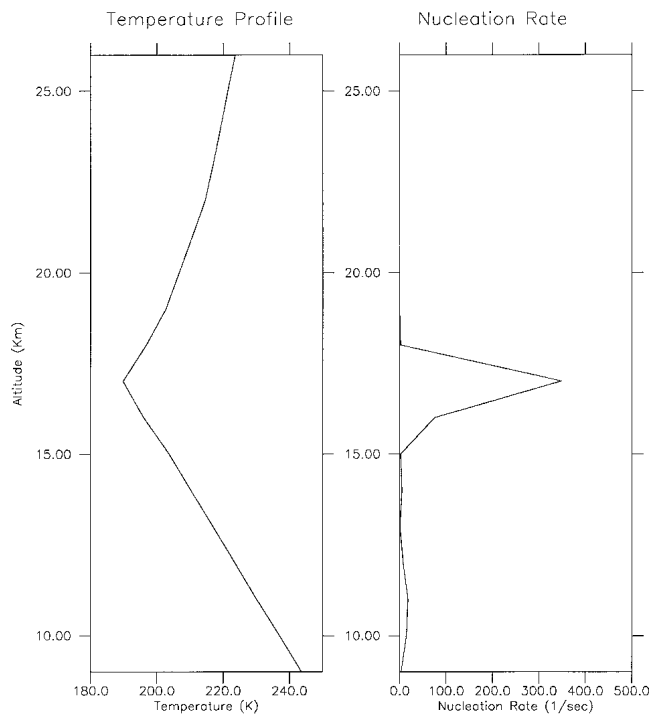


FIG. 2. The left-hand panel shows the temperature profile assumed for the tropical region and used to calculate the nucleation rates shown in the right-hand panel.

ecules, but that value is subject to great uncertainty.) Significantly larger nucleation rates are obtained if the temperature is a few degrees colder or if the sulfuric acid concentration is larger. Details of the nucleation rate calculation used are given in appendix A.

To determine the actual number of particles formed in the ascending air mass would require a careful study involving the depletion of molecules due to nucleation and growth processes. Those mechanisms were included in the nucleation studies of Zhao et al. (1995a) but for different conditions than those considered here. We have not carried out a similar study because we are only interested in identifying regions of the atmosphere where particle formation is favored. The actual number of new particles is not particularly important for our purposes and would be highly dependent on the theory of homogeneous heteromolecular nucleation, which has not been well validated. However, most researchers agree that the theory can be used to identify regions where particle formation is favored. In spite of these caveats, it might be mentioned that measurements reported by Brock et al. (1995) indicate aerosol number mixing ratios of 10^4 mg^{-1} air at the tropical tropopause. This corresponds to about

7×10^4 particles cm^{-3} at 16 km, which is close to the value obtained from our nucleation rate calculation.

It should be pointed out that the homogeneous nucleation of sulfate particles in the upper troposphere at *midlatitudes* is negligible. Hamill et al. (1982) showed that in the midlatitude troposphere the homogeneous nucleation rate ranged from a bit less than unity at 10 km down to less than 10^{-5} s^{-1} at the tropopause.

As can be appreciated from Fig. 2, even in the equatorial region the nucleation rate is small except at the coldest temperature. However, at the temperature minimum, the nucleation rate is so large that essentially every sulfuric acid molecule is transformed into a tiny but stable particle containing about 10 water molecules for every sulfuric acid molecule. Initially these clusters contain a single sulfuric acid molecule and have a radius of about 5 Å. One might reasonably ask whether this is really “nucleation” or merely a hydration process. The end result, however, is the same, in that small stable clusters of $\text{H}_2\text{SO}_4\text{-H}_2\text{O}$ are formed homogeneously.

b. Coagulation

The newly nucleated particles can be assumed to very quickly coagulate to form larger particles. As mentioned above, the question arises whether the presence of ice crystals in the nucleating air mass will result in a scavenging of newly nucleated particles or whether the particles will primarily coagulate with one another.

In Fig. 3 we illustrate the coagulation of newly nucleated particles in the presence of ice crystals of about $10 \mu\text{m}$ radius having a number density of 0.01 cm^{-3} . In this and the subsequent figure we present a large number of size distributions on the same plot. The vertical lines are the initial monodisperse size distributions of sulfuric acid solution droplets and ice crystals. As time goes on, coagulation changes the monodisperse size distributions, as shown. The vertical lines are initially transformed into steeply sloped nearly straight lines, then gradually the number density at the smallest size decreases, and the size distribution becomes curved and peaked at a larger size. The figure shows the results of coagulating for 100 000 s (somewhat over 1 day).

The presence of ice particles has no significant effect on the development of the size distribution of the small (sulfate) particles; that is, the size distri-

bution obtained assuming no ice crystals is essentially undistinguishable from that of Fig. 3. However, we found that if the number density of ice crystals increases, they do begin to have a significant effect on the newly nucleated sulfate particles. For a number density of 10 ice crystals cm^{-3} of $10\text{-}\mu\text{m}$ radius, the scavenging is so great that within a few hours there are essentially no small sulfate particles left.

To illustrate the development of a size distribution by the coagulation of newly nucleated particles we carried out a coagulation calculation, as shown in Fig. 4, for initially monodisperse aerosols with number concentrations of 10^5 cm^{-3} and 10^7 cm^{-3} . In neither case are any large particles present. (In other words, no ice crystals are present.) We note that in both cases, the monodisperse distribution quickly broadens and develops into a size distribution resembling that of stratospheric aerosols, except for the mode radius being quite small, of the order of $5 \times 10^{-7} \text{ cm}$ or $0.005 \mu\text{m}$ for the initial concentration of 10^7 cm^{-3} . The mode radius is even smaller for the initial concentration of 10^5 cm^{-3} . The total coagulation time in both cases was about one day. After this time the changes in the size distribution are quite small. For example, allowing the particles to coagulate for 5 days yields a size distribution very similar in appearance but with a mode radius of $0.008 \mu\text{m}$, and after 21 days the

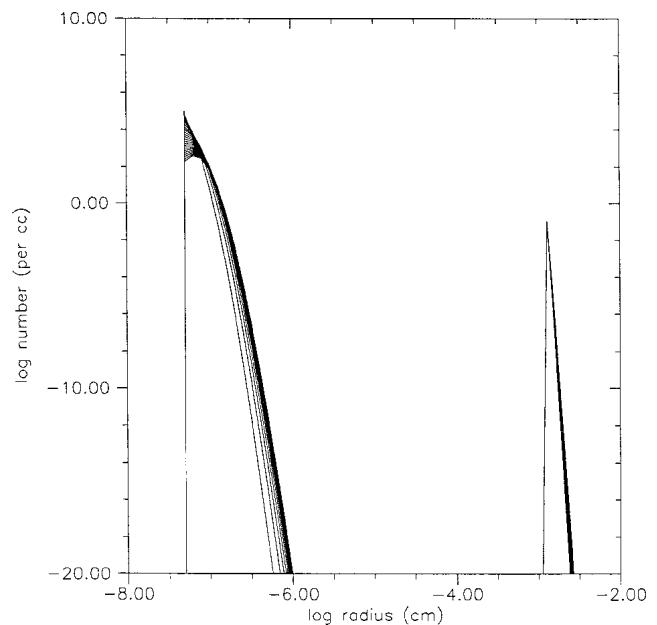


Fig. 3. Change in size distribution of an initially monodisperse aerosol having a radius of 5 Å and a number density 10^5 cm^{-3} in the presence of particles having a radius of about $10 \mu\text{m}$ and a number density 0.01 cm^{-3} .

mode radius is $0.010 \mu\text{m}$. However, it is doubtful that an air parcel will maintain its identity beyond a few days at most. We consider the mixing of air parcels below. For details of the coagulation calculation, see appendix B.

We conclude that a rising air mass, crossing the tropopause, will carry with it a collection of sulfate particles having a size distribution somewhat as presented in Fig. 4. This air mass will warm up as it rises due to diabatic heating in the Tropics (see the temperature profile of Fig. 2). If ice crystals are present in the air mass, they will evaporate. The mass of these ice crystals is so small that they do not significantly hydrate the stratosphere. If we assume a density of ice crystals of 0.1 cm^{-3} having a radius of $10 \mu\text{m}$, then some 1.2×10^{13} molecules of water per cubic centimeter of air are transported into the stratosphere. The number of air molecules at 18 km is about $2.9 \times 10^{18} \text{ molecules cm}^{-3}$. Therefore, if all of the water from these ice crystals is deposited into the stratosphere, the mixing ratio of water in this air will be about 4.3 ppmv. This is the right order of magnitude for stratospheric water vapor, indicating that our proposed mechanism is not inconsistent with the measured amounts of water vapor in the lower tropical stratosphere.

As the parcel rises, the ambient temperature increases and as a result the composition of the par-

ticles changes. Interestingly, the particles will grow smaller by losing water to the environment, since a sulfate solution must become more concentrated in sulfuric acid to maintain equilibrium when the temperature rises (Steele and Hamill 1981). This is a very small effect and probably not observable. The water released into the environment does not appreciably change the water content of the stratosphere; at most this process releases about 3×10^{-5} ppmv of water to the stratosphere.

As the parcel moves about in the stratosphere, the particles will continue to coagulate, but soon coagulation becomes less and less important and the principal growth mechanism is heteromolecular condensation. We consider this process in detail in the next section.

3. The growth of aerosol particles by condensation

In the last section we considered the processes of nucleation, which generated an aerosol of very small particles, and coagulation for 1 day, which formed the size distribution illustrated in Fig. 4. Allowing the coagulation routine to run for longer time periods, such as 30 days or even 100 days, has a slight effect on the size distribution, but in general the most important effects of coagulation are terminated within a few days. For example, we find, after running the coagulation program for 30 days, that for an initial monodisperse size distribution of $10^5 \text{ particles cm}^{-3}$ we obtain a size distribution that peaks at a radius of $3.2 \times 10^{-7} \text{ cm}$. The total number of particles at that time is about 330 cm^{-3} . Going to an extreme case, assuming the monodisperse size distribution starts with $10^7 \text{ particles cm}^{-3}$ the size distribution ends up with a peak at $1.6 \times 10^{-6} \text{ cm}$ and the total number of particles is about 200 cm^{-3} . These particles are too small to be observed by most particle-measuring devices, but the large number densities do agree with observations made near the tropical tropopause by the University of Denver Condensation Nuclei Counter (Brock et al. 1995).

The H_2SO_4 concentration in the upper tropical troposphere is not known, but if it lies in the range of 10^4 – $10^7 \text{ molecules cm}^{-3}$, this is at most 10^{-15} of sulfate aerosol cm^{-3} . But we know that the background aerosol has a mass of about $10^{-13} \text{ g cm}^{-3}$. That is, even if the amount of sulfuric acid involved

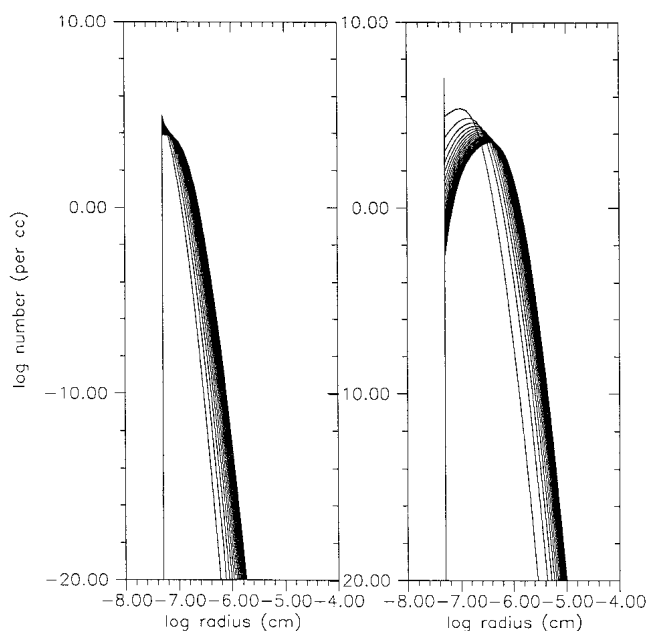


FIG. 4. Change in size distribution of an initially monodisperse size distribution for an initial number density of $10^5 \text{ particles cm}^{-3}$ (left panel) and $10^7 \text{ particles cm}^{-3}$ (right panel). The total coagulation time in both cases is 10^5 s (about 1 day).

in the nucleation is several orders of magnitude greater than we assumed, there is still not enough mass of sulfate to account for observations. The extra mass must come from the condensation of H_2SO_4 produced in the stratosphere from the oxidation of SO_2 and COS. See Turco et al. (1979) for details of sulfur chemistry in the stratosphere.

We now consider the growth of these newly formed particles. They grow by the condensation of both water vapor and sulfuric acid vapor. The growth of a solution particle by heteromolecular condensation is described in Hamill (1975) and outlined briefly in appendix C. We apply this theory to the particle size distribution of Fig. 4 (left-hand side).

We allowed the particle size distribution of the left-hand side of Fig. 4 to continue coagulating at a slightly higher temperature (205 K) for a period of 104 days. This yielded the size distribution on the extreme left of Fig. 5. We then allowed the particles to both grow and coagulate for another 50 days, and the size distribution changed as indicated by the other curves in Fig. 5. (The curves are sepa-

rated from one another by periods of 400 h, about 17 days.)

The effect of coagulation is not nearly as important in changing the size distribution as the growth process. In fact, if we neglect coagulation, we obtain curves that are essentially indistinguishable from those in Fig. 5. Note that growth by condensation appears to lead to a “narrowing” of the size distribution. This is, of course, merely an artifact of the logarithmic scale. Growth by condensation essentially causes particles of all sizes to increase equally in radius, so actually, the size distribution has the same “width” at all times. However, the result obtained in Fig. 5 differs significantly from the size distributions that are observed in the stratosphere, which are much “wider” and peak at a much larger radius. For example, a lognormal size distribution with a mode radius (r_m) of $0.0725 \mu\text{m}$ and a geometric mean standard deviation (σ) of 1.86 (canonical stratospheric values) has the appearance indicated in Fig. 6. The equation for this curve is

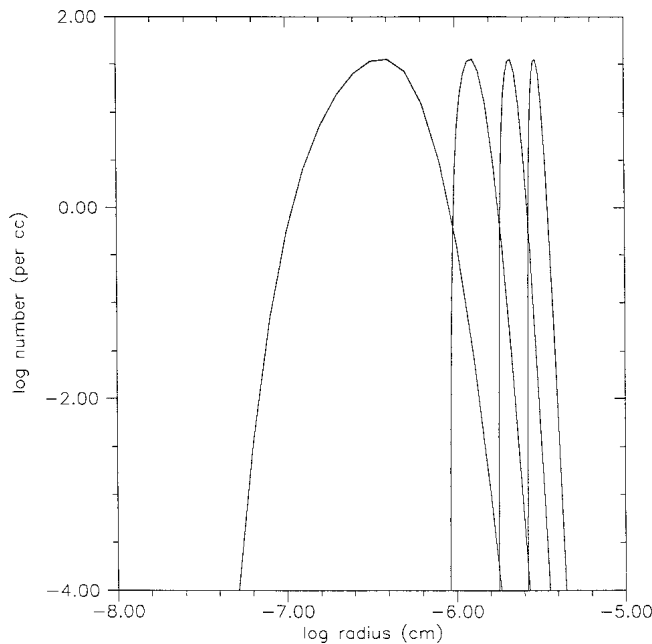


FIG. 5. Change in size distribution of an initially monodisperse aerosol with 10^5 particles cm^{-3} . The first curve on the left is the size distribution formed by coagulation alone for 104 days. The other curves are due to both coagulation and condensational growth. The curve on the far right is the result after an additional 50 days of both coagulation and growth. In carrying out the calculation it was assumed that the sulfuric acid concentration was 8.8×10^5 molecules cm^{-3} and there was always sufficient water vapor to maintain equilibrium with a 75% H_2SO_4 (by weight) solution particle.

$$\frac{dN(r)}{dr} = \frac{N_o}{r \ln \sigma_g} \frac{1}{(2\pi)^{1/2}} e^{-\frac{1}{2} \left[\frac{\ln r - \ln r_m}{\ln \sigma_g} \right]^2} \quad (1)$$

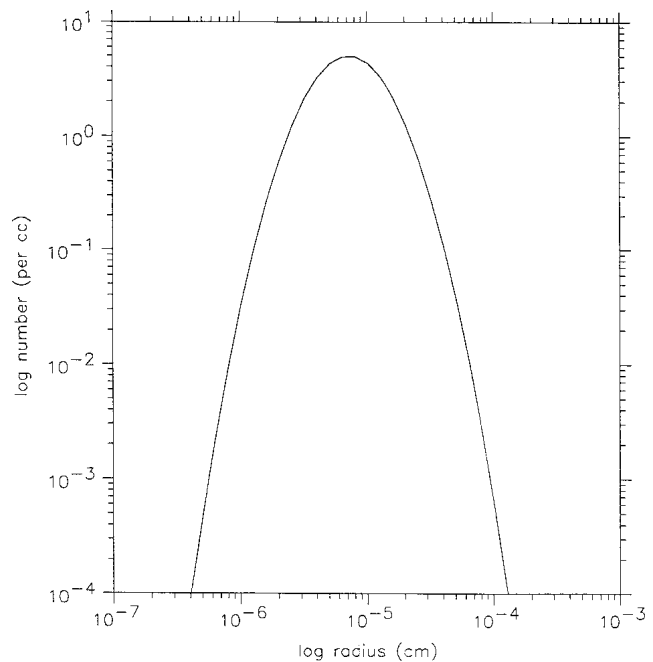


FIG. 6. A lognormal distribution given by Eq. (1) with $N_o = 30$, $r_m = 0.0725 \mu\text{m}$, and $\sigma = 1.86$.

The reason our curves do not resemble the observed stratospheric size distributions (which are reasonably well modeled by the curve of Fig. 6) is that we have ignored the fact that the air parcel mixes with air that has been in the stratosphere for longer periods of time. To simulate this process requires a much more sophisticated model than we are using here; however, we can get a rough estimate of the effect of mixing by allowing our aerosol to evolve via condensational growth and coagulation and obtaining a large number of size distributions as a function of time, such as presented in Fig. 5. We “mixed” these size distributions by adding them to each other and normalizing appropriately. This, however, did not lead to a reasonable size distribution because we had neglected the fact that an aged size distribution will be affected by sedimentation. Therefore, before adding our size distributions together, we allowed the larger particles to fall out of the older size distribution. This admittedly crude attempt to generate a physically reasonable size distribution from the initial monodisperse aerosol led to the result shown in Fig. 7. This represents the aerosol in an air parcel that has been mixed with other air parcels containing particles that were created up to 2 yr previously. Although the resultant size distribution does not have the symmetry of the lognormal distribution, it is based on physically

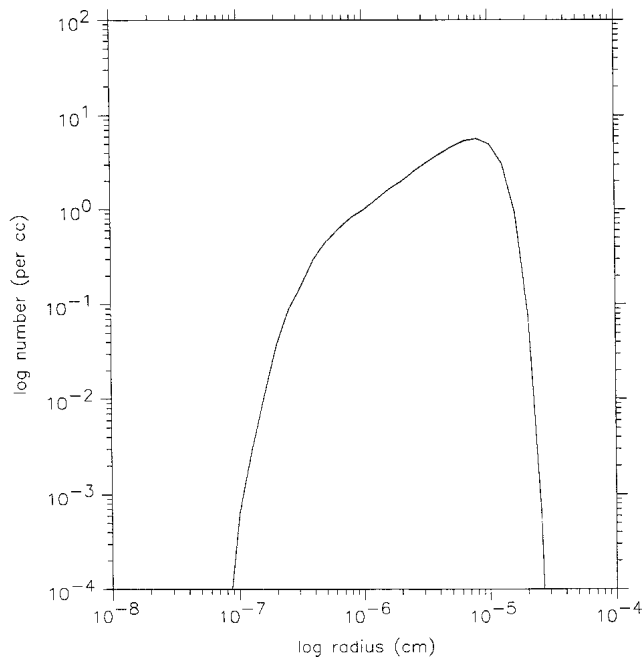


FIG. 7. The size distribution obtained by allowing the aerosol particles to coagulate, grow, sediment, and mix with other air parcels.

sound assumptions and is reasonably close to observed distributions (as in Fig. 6).

As mentioned above, the aerosol parcel we are considering will eventually be transported out of the tropical regions to higher latitudes. An aged size distribution, such as illustrated in Fig. 7, is more likely to be found at midlatitudes than in the Tropics, in agreement with observations by Goodman et al. (1982) and Brock et al. (1995).

Assuming the size distribution of Fig. 7, let us enquire into the behavior of the aerosol as a function of time. As we know, there will be a slow growth of all particles and a sedimentation of the larger particles. Both of these processes are relatively slow. The aerosol will respond much more rapidly to changes in the temperature, by either absorbing or evaporating water. Physically, the reason for this is the fact that there is much more water vapor than sulfuric acid vapor in the stratosphere. A binary solution droplet will not, in general, be in equilibrium with both vapors. Since the number of collisions of water molecules with the droplet exceeds the number of collisions of sulfuric acid molecules with the droplet by a factor of about 10^7 , the sulfate aerosol particles quickly come to equilibrium with respect to water. They are, however, “undersaturated” with respect to sulfuric acid, so every sulfuric acid molecule incident on an aerosol particle will be absorbed.

Changes in temperature affect the equilibrium vapor pressure of water in a binary solution, and the aerosol particles will either absorb or evaporate water molecules in such a way as to maintain an equality between the vapor pressure in the binary solution and the partial pressure of water molecules in the environment. This process has been described in detail in Steele and Hamill (1981). Of interest to us is the response of the aerosol on an annual basis as the temperature of the stratosphere varies. The annual variation in temperature at 22-km altitude and 40°N latitude can roughly be described by the formula

$$T = 114.4 + 5 \sin\left(\pi \frac{t}{365}\right), \quad (2)$$

where t is the day of the year. The stratosphere warms up in summer and cools in winter, as one might expect. As the temperature decreases, the droplet can maintain equilibrium with the environmen-

tal water vapor only by growing more dilute, that is, by absorbing water molecules. Therefore, the particles will grow larger in winter and will shrink somewhat in summer. This fact explains the observed changes in optical depth with season that were noted in the SAGE II data by McCormick et al. (1993). In Fig. 8 we show the temperature as a function of time, as given by the formula above, and the corresponding change in the extinction due to the growth–evaporation of the droplets, assuming the initial size distribution is that of Fig. 7. We also present optical depths in the 40°–45° latitude range as obtained by summing the SAGE II extinctions from 2 km above the tropopause to 40 km. The calculated extinctions at a particular altitude do not show such good agreement with the measured extinctions because of dynamical processes and short-term temperature changes that we cannot model; nevertheless, it is clear that the seasonal variations in extinction are in reasonable agreement with the optical depths obtained from SAGE II measurements. A detailed study of changes in the SAGE II optical depths as a function of time was carried out by Yue et al. (1991).

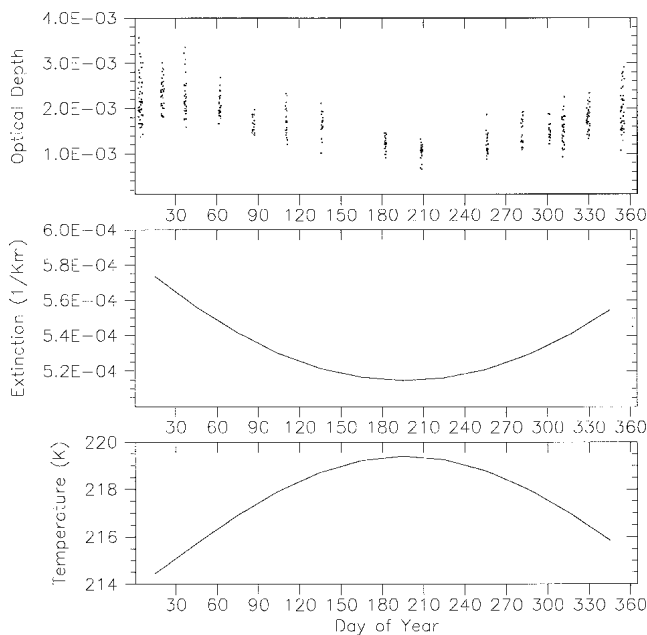


FIG. 8. (top) The optical depth as a function of day of year as evaluated from the SAGE II dataset for 1989 between the latitudes of 40.0° and 45.0°N. This was evaluated by summing extinctions from 2 km above the tropopause to 40 km. Gaps are due to the satellite observation point being at a different latitude. (middle) A model calculation of extinction as a function of day of year for an aerosol at midlatitudes in the Northern Hemisphere. The aerosol particles absorb and evaporate water as the temperature changes with season. (bottom) The assumed change in temperature used in the calculation of extinction.

It is interesting to note the variation in the characteristics of the stratospheric aerosol as a function of latitude. In Fig. 9 we present the extinction ratio profiles obtained by the SAGE II instrument in various latitude bands. (The extinction ratio is the ratio of aerosol extinction to molecular extinction.) The figure shows that the aerosol layer not only descends in altitude as it moves to higher latitudes but also a significant decrease in the extinction ratio, which has a maximum value of about 7 in the 0°–10° latitude range and a maximum value of less than 4 in the 50°–60° range. It is easy to show that the descent of the layer with latitude is steeper than lines of constant potential temperature, indicating that the aerosol is in some respect a tracer for the general circulation.

4. Removal processes

a. Isentropic transport

Ignoring diabatic processes, Chen et al. (1994) studied the dispersion of an equatorial ideal tracer for two 5-month periods, namely 1 June to 31 October 1994 and 1 December 1992 to 30 April

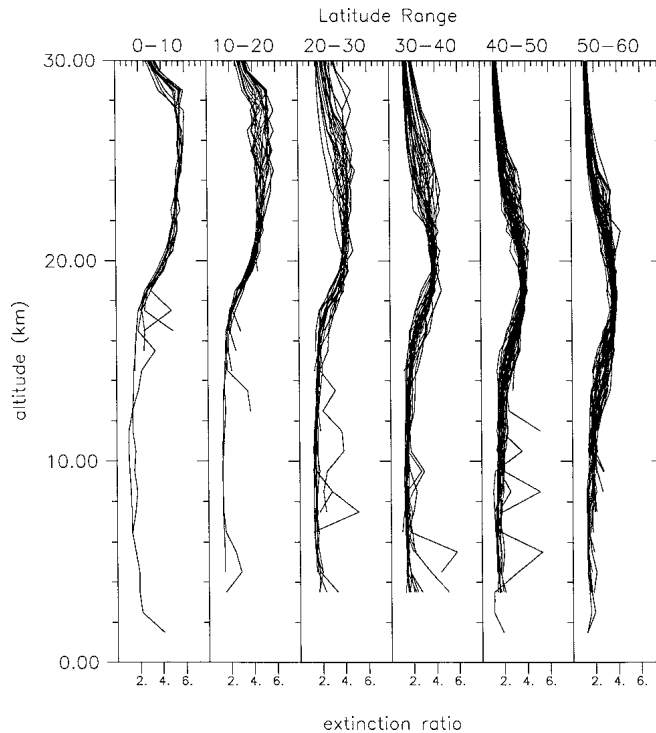


FIG. 9. Extinction ratios from the SAGE II satellite system in various latitude ranges. The extinction values were measured in April 1989 in the Southern Hemisphere. We have removed extinction ratios greater than 7 at lower altitudes for these are indications of tropospheric clouds.

1993. This analysis of the isentropic mass exchange between the Tropics and extratropics showed that at the 400-K level (about 17 km in the Tropics) there was considerable meridional mixing into the winter midlatitudes during the 5-month period but less mixing at the 600-K level (about 25 km in the Tropics). Chen et al. conclude that the process of mixing from the Tropics to mid- and high latitudes is due to large-scale Rossby waves that pull large-scale “tongues” of material from the Tropics, which are then mixed irreversibly with midlatitude air by the wave-breaking process in the “surf zone” in the subtropics. Trepte et al. (1993) in an analysis of the Mt. Pinatubo volcanic aerosols used the SAGE II dataset to show that in a region of several kilometers above the tropopause there is a rapid poleward transport of aerosols to the midlatitudes.

In an excellent review paper, Holton et al. (1995) describe stratospheric–tropospheric exchange processes as due to a global scale “fluid-dynamical suction pump” driven by Rossby waves. This pump draws air upward from the tropical lower stratosphere, then poleward and downward into the extratropical troposphere. For example, an air mass at 400 K in the Tropics (about 17 km) can be transported to higher latitudes, then descend to a lower altitude, crossing isentropic surfaces. (This process would be accompanied by diabatic cooling.) If the descent occurs at, say, 50°N, the air mass could descend to between 9 and 15 km and still be in the stratosphere. However, the potential temperature would be in the 300–380-K range. If the air mass now moves isentropically toward the equator, it will cross the tropopause. Once the air mass is in the troposphere, the sulfate aerosols will be very quickly removed. An estimate by Rosenlof and Holton (1993) (cited in Holton et al. 1995) indicates that on the annual mean, $85 \times 10^8 \text{ kg s}^{-1}$ of air are transported across the tropopause from the stratosphere in the extratropics. There is somewhat more exchange in the Northern Hemisphere than in the southern extratropics with fluxes of $53 \times 10^8 \text{ kg s}^{-1}$ and $32 \times 10^8 \text{ kg s}^{-1}$ respectively. These fluxes lead to a stratospheric residence time of approximately two years.

The actual mechanism of the exchange process is well described by Appenzeller and Davies (1992), who show that stratospheric intrusions into the upper troposphere by isentropic flow usually take the form of long thin streamers (some 2000 km long by 200 km wide). The flow is isentropic and

in the general direction of the Tropics. These intrusions are usually associated with the development of a low pressure system and a cold front at the surface. Such a streamer will develop a train of vortices along its sides and the tip will split or roll up. In these smaller-scale structures there is local and irreversible but isentropic mixing of stratospheric air into the troposphere. When the tip of the streamer rolls up, it is referred to as a “cut-off” cyclone. The mixing of stratospheric air caused by cutoff cyclones is probably less significant to stratosphere–troposphere exchange than the mixing through “tropopause folds” that develop as the high-latitude stratospheric air moves in long tongues toward the Tropics (Price and Vaughan 1993).

b. Cloud intrusions into the stratosphere

In Fig. 10 we show a set of vertical profiles of aerosol extinction as observed by the SAGE II instrument. The figure is a composite of all the extinction measurements made by SAGE II at sunrise during 8 and 9 April 1989. The measurements were clearly midlatitude values with the latitude ranging from 40° to 45°S. The figure indicates that above about 16 km (about 100 mb) the aerosol layer is reasonably uniform; that is, the various extinction profiles are enclosed in a reasonably narrow envelope. However, below about 16 km the situation is quite different, and there is a large amount of variation between one profile and the next. For these profiles the reported tropopause in all cases lay between 10 and 14 km. Note that the peak of the layer is several kilometers above the tropopause. The fact that the layer decays as one goes down in altitude toward the tropopause suggests it is being “eaten away” from below. Looking at individual profiles it is clear that in some cases cloud layers are above the reported tropopause. This figure implies that a possible midlatitude removal process involves the incursion of cloud tops into the stratosphere.

An interesting radar scan of a thunderstorm near Huntsville, Alabama, was obtained by V. Chandrasekhar of Colorado State University on 28 July 1986. This is presented in Fig. 11. Note that the radar echoes extend up to 18-km altitude. A study of the meteorological data contained in the SAGE II dataset shows that the tropopause in late July at the latitude of Huntsville can be expected to be in the range of 15–17 km. Although

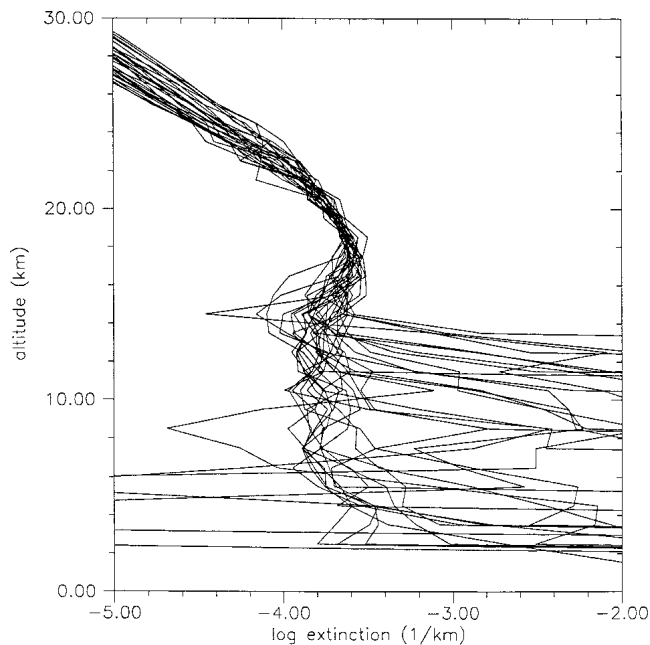


FIG. 10. A composite of all extinction measurements made by SAGE II in latitude range 40° – 45° S on 8 and 9 April 1989 illustrating the great variability in extinction below about 16 km.

an 18-km tropopause is somewhat unusual, they do occur occasionally at that latitude. Nevertheless, it is possible that the storm pictured here did pierce the tropopause. In that case, the mixing of stratospheric and tropospheric air would be an efficient removal mechanism for sulfate aerosols near the the tropopause.

It should be noted, however, that there are alternate explanations for the fact that the peak of the aerosol layer lies several kilometers above the tropopause. For example, this could be due to tropical air close to the tropopause moving to midlatitudes and carrying with it younger and smaller particles. Nevertheless, particle entrainment into clouds or diabatic stratosphere–troposphere exchange processes related to large storm systems do appear to be reasonable removal mechanisms for sulfate particles in the lower stratosphere.

c. Sedimentation

The particles residing in midlatitudes will slowly grow by the process of heteromolecular condensation as described above, and some of them

will grow large enough to sediment out of the stratosphere. We have carried out calculations to evaluate the residence time of an aerosol particle in the stratosphere. The result depends, of course, on the particular history of the aerosol, that is, whether or not it is in a region of where there is significant sulfuric acid production from SO_2 , leading to rapid growth, or in a region where there is little sulfuric acid and very slow growth. However, we can get an idea of the residence time of the aerosol particles by assuming the size distribution of Fig. 7 and evaluating the fall velocity for conditions equivalent to 22-km altitude and 220-K temperature. We obtain fall speeds of the order of $1.0 \times 10^{-3} \text{ cm s}^{-1}$ for particles of radius $0.06 \mu\text{m}$ and of the order of $5.0 \times 10^{-3} \text{ cm s}^{-1}$ for particles of radius $0.25 \mu\text{m}$. At these rates, it would require 6.3 yr and 1.3 yr, respectively, for these particles to fall 2 km to an altitude of 20 km. Thus the sedimentation of aerosol particles is not an effective removal mechanism, except for the very few particles that somehow survive long enough in the stratosphere to grow to large sizes (i.e., an appreciable fraction of a micron in radius).

d. Polar vortex

During the winter months, a fairly strong vortex is set up in the polar regions, especially over Antarctica. As the air cools (due to a lack of sunlight), it descends and it contracts. Since the angu-

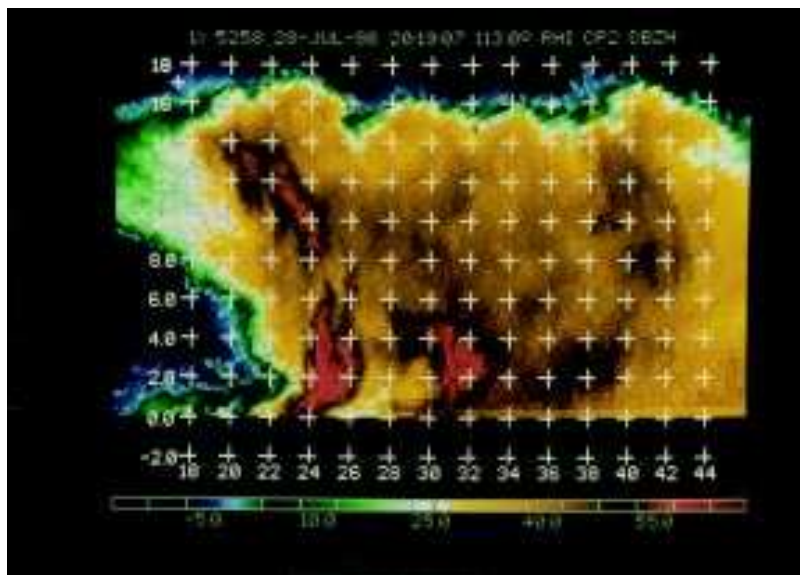


FIG. 11. Radar scan of a thunderstorm near Huntsville, Alabama, on 28 July 1986. The horizontal scale is km from the radar; the vertical scale is km above the surface. The color scale is in db. Courtesy of V. Chandrasekhar.

lar momentum of the air must be conserved, it speeds up, much as an ice skater's spin speeds up when she pulls her arms in to her sides. The rotating air mass is rather well isolated from air at lower latitudes outside of the vortex, as can be appreciated from studies of tracer chemicals inside and outside of the vortex (Profitt et al. 1989).

The Antarctic polar vortex is roughly bounded by a 60°S latitude circle (Loewenstein et al. 1989). From the Stratosphere Aerosol Measurement (SAM) II dataset one finds that a large fraction of the aerosol particles in the Antarctic stratosphere are removed during the winter season and a smaller but still significant fraction are removed from the Arctic winter stratosphere (McCormick et al. 1981). The amount of stratospheric air enclosed in the vortex is, approximately, 1/16 of the total stratospheric air. If all of the aerosol particles in this air mass are removed annually and if an equal amount is removed in the northern vortex, then the lifetime of a stratospheric aerosol particle would be about 8 yr. This means that even assuming a maximal amount of removal through the polar vortices, the loss is only about one-fourth as great as that due to mixing across the tropopause at midlatitudes.

5. Conclusions

We have illustrated the fact that the life cycle of the background stratospheric sulfate aerosol is reasonably well understood. The particles are probably formed in the tropical tropopause or lower stratosphere and then are carried to higher altitudes by ascending air. There they will generate the expected size distribution by coagulation, growth by condensation, and mixing with older aerosols. Eventually the particles will migrate to mid- and high latitudes where they will be removed from the stratosphere by a variety of different processes. These removal processes need to be further quantified, but it appears reasonable to assume that isentropic mixing across the tropopause, primarily through tropopause folds, is the major removal process.

Appendix A: The nucleation calculation

In this appendix we present a detailed description of the nucleation rate calculation, which is

assumed to proceed via the homogeneous nucleation of binary solution droplets composed of H_2SO_4 and H_2O . A binary system droplet can exist under thermodynamic conditions that would lead to the evaporation of either of the pure substances. This is because the vapor pressure of a component in solution is less than the vapor pressure of the pure substance. For example, in the stratosphere we find sulfuric acid solution droplets existing under conditions that would not allow for the presence of either pure water droplets or pure sulfuric acid droplets. In fact, since the water content of the stratosphere is about 5 ppmv, at 220 K the relative humidity is less than 0.5%; therefore, a pure water droplet in the stratosphere would evaporate immediately. However, water in a sulfuric acid solution droplet is stable.

Reiss (1950), Doyle (1961), Kiang and Stauffer (1973), and others considered the problem of the nucleation of a binary system. Hamill et al. (1977) applied the theory to the formation of sulfuric acid solution particles in the stratosphere. They found that homogeneous binary nucleation under normal stratospheric conditions is negligible.

The theory of binary homogeneous nucleation is based on the fact that for a solution the increase in Gibbs free energy in forming a liquid droplet from the vapor is given by

$$\Delta G = -n_A kT \ln \frac{P_A}{P_A^o} - n_B kT \ln \frac{P_B}{P_B^o} + 4\pi r^2 \sigma, \quad (\text{A1})$$

where $P_{A,B}^o$ are the vapor pressures of A, B for a flat solution having the same composition as the droplet, and $P_{A,B}$ are the partial pressures of these substances in the environment (given by $P_A = N_A kT$). The quantities n_A and n_B are the number of molecules of A and B in the droplet, r is the radius of the droplet, and σ is the surface tension of the solution.

This relationship assumes the droplet is a sphere of radius r and that the droplet has a surface tension σ . Both of these assumptions are dubious when applied to a cluster of a few molecules.

The equation for ΔG shows that for very small droplets (embryos) the positive surface energy term (the last term) will dominate, because it is proportional to the square of radius. The first two terms depend on the number of molecules in the droplet and hence depend on the volume, that is, on the

cube of the radius. Therefore the negative terms will dominate at larger values of r . That is, the Gibbs energy difference ΔG goes through a maximum. Let the radius of the droplet at this maximum be r^* (the “critical radius”). This implies that embryos smaller than r^* will tend to evaporate, whereas embryos larger than r^* will tend to grow. Therefore, if $r > r^*$, the embryo is stable.

If one assumes a steady-state embryo size distribution is set up by random molecular collisions, then the nucleation rate can be defined as the rate at which critically sized embryos are produced. This rate is given by

$$J = 4\pi r^{*2} \beta_A N_B \exp\left(-\frac{\Delta G^*}{kT}\right), \quad (\text{A2})$$

where β_A is the rate at which A molecules (sulfuric acid molecules) impinge upon a critically sized embryo and N_B is the number of water molecules per unit volume in the environment.

We evaluated the nucleation rate using the best known values for the vapor pressure and other parameters. Analyzing the results, we found that the calculation of J for the coldest temperatures led to values of n_A less than unity. Obviously, the smallest stable clusters must contain at least one sulfuric acid molecule, so we conclude that the theory is predicting that every sulfuric acid molecule is forming a stable cluster. The stable cluster will then grow by absorbing water and sulfuric acid molecules (condensation). However, if all H_2SO_4 molecules form stable clusters, then the initial growth process is via coagulation, not condensation. Nevertheless, the stable embryo can absorb water molecules, and we assume that this process does take place until the cluster reaches a composition such that it will be in equilibrium with water vapor. This process is discussed in detail in Steele and Hamill (1981). For temperatures of around 190 K, a stable cluster in thermodynamic equilibrium with water vapor in the environment will have about 10 water molecules for each sulfuric acid molecule. The smallest such clusters have a radius of about 5 Å.

There has been a great deal of criticism leveled at the theory of binary homogeneous nucleation, and many of the criticisms are valid. We do not know whether or not the predictions of the theory are valid because there have been no convincing

experimental verifications of the theory. However, it is the only theory presently available, although there is work being carried out to develop a kinetic theory of binary system nucleation. In defense of the theory, we might say that the nucleation rates obtained may not be valid, but the theory can be used to estimate places or conditions where nucleation is likely to occur.

Appendix B: The coagulation calculation

We now discuss the technique used to evaluate the coagulation of the newly formed aerosol particles. For a fuller discussion see Hamill et al. (1977). The basic idea is to discretize the particle size distribution by assuming that all the particles in a given size range have the same radius. That is, all the particles with radii between r and $r + dr$ are assumed to be of the same size. We set up a size distribution by defining a set of radii (we normally use 40 bins). These are selected by determining the smallest particle size. The volume of the smallest particles is determined, and this defines the first (or smallest) bin. The remaining bins are determined by requiring that they represent particles whose volume is twice the volume of those in the previous bin. That is, particles in bin i have a radius $r_i = r_1(2)^{(i-1)/3}$, where r_1 is the radius of the particles in the smallest bin.

Let n_i be the number of particles in the i th bin. Then, the rate of change of n_i is given by (Fuchs 1964)

$$\frac{dn_i}{dt} = -n_i \sum_{j=1}^{\infty} K_{ij} n_j + \frac{1}{2} \sum_{j=1, k=i-j}^i K_{kj} n_k n_j, \quad (\text{B1})$$

where the “coagulation kernel” K_{ij} is given by

$$K_{ij} = 2\pi r_{ij} D_{ij} \left(\frac{r_{ij}}{r_{ij} + \delta_{ij}} + \frac{4D_{ij}}{G_{ij} r_{ij}} \right)^{-1}. \quad (\text{B2})$$

In this last equation the quantity r_{ij} is the sum of the radii of particles in the i th and j th bins, that is, $r_{ij} = r_i + r_j$. Similarly, the other symbols with double indices are the sums of the quantities, evaluated for bins i and j ,

$$D = kTB = kt \frac{1}{6\pi\eta r} \left(1 + 1.246\text{Kn} + 0.42\text{Kne}^{\frac{-0.87}{\text{Kn}}} \right), \quad (\text{B3})$$

$$\delta = \frac{1}{6rl_b} \left[(2r + l_b)^3 - (4r^2 + l_b^2)^{\frac{3}{2}} \right] - 2r, \quad (\text{B4})$$

$$G = \left(\frac{8kT}{\pi m} \right)^{\frac{1}{2}}, \quad (\text{B5})$$

where $l_b = 8D/\pi G$ and Kn is the Knudsen number defined by $\text{Kn} = r/\lambda$ with λ being the mean free path in air.

In generating Fig. 4 we began by assuming that only the first bin was populated. This monodisperse size distribution is therefore represented by a vertical line. During the first time step, there will be a certain number of collisions between these particles. They will generate particles in bin 2 having twice the volume of particles in bin 1. The number of such particles formed will be equal to the number of collisions. During the next time step there will be collisions between bin 2 particles forming particles that have the volume of bin 3. However, there will also be collisions between bin 1 and bin 2 particles and these will be too large for bin 2 and too small for bin 3. They are distributed proportionally between the two bins in such a way as to conserve mass.

At each time step we generate a size distribution. These look like a log normal size distribution. In Figs. 3 and 4 we only drew a few of the size distributions obtained. By considering curves from left to right, one can get a general idea of the time evolution of the size distribution. In producing Fig. 3 we also allowed for the coagulation of all particles with larger ("ice crystal") particles.

Appendix C: Heteromolecular condensation

The growth of a binary system droplet by condensation is discussed in detail in Hamill (1975). The basic idea is that a binary system droplet can achieve equilibrium with the vapor phase of one of its components but not, in general, with both. In the specific case of a sulfuric acid solution droplet in the stratosphere, there will be equilibrium

with respect to water, but not with respect to sulfuric acid. This is simply due to the fact that there is so much more water than sulfuric acid in the stratosphere. It can easily be demonstrated that in general the sulfuric acid vapor pressure in a stratospheric sulfate particle is less than the sulfuric acid vapor pressure $P_s = n_s kT$ (where n_s is the number of sulfuric acid molecules per unit volume in the environment; we let the subscript "s" refer to sulfuric acid and the subscript "w" refer to water). Under these circumstances, any sulfuric acid molecules incident on the particle will be absorbed. The absorption of sulfuric acid will change the composition of the droplet (it becomes more acidic) and, consequently, the vapor pressure of water in the droplet also changes. The water is then no longer in equilibrium with the environment (the vapor pressure of water P_w^0 is now less than the partial pressure of water, $P_w = n_w kT$). To regain equilibrium, the droplet will absorb some water from the environment. Hence, the process of growth by heteromolecular condensation consists of a series of states in which water equilibrium is maintained, interrupted by the absorption of sulfuric acid molecules. Clearly, the rate determining factor is the number of sulfuric acid molecules absorbed per second. If the sticking coefficient is assumed to be unity, this is just the rate at which sulfuric acid molecules impinge on the particle. The impinging rate is given by kinetic theory as

$$\beta_s = n_s \left(\frac{kT}{2\pi m_s} \right)^{\frac{1}{2}}. \quad (\text{C1})$$

The growth of a sulfate aerosol particle by heteromolecular condensation depends on the difference between the vapor pressure of sulfuric acid in the droplet and the environmental partial pressure of sulfuric acid, that is, on the quantity $P_s - P_s^0$. As is well known, the growth by condensation depends on the diffusion of gases to the surface of the particle and the growth rate dr/dt is inversely proportional to the radius of the particle. However, as shown by Hamill et al. (1977), for particles smaller than about 0.2- μm radius, the growth rate is essentially linear in β_s and is given by

$$\frac{dr}{dt} = \frac{\bar{v}\beta_s}{\chi}, \quad (\text{C2})$$

where \bar{v} is the average volume per molecule in the drop and $\chi = n_s/(n_s + n_w) =$ concentration of acid in droplet. We used Eq. (C2) in our evaluation of growth rates in this paper.

It should be mentioned that if the temperature increases sufficiently (to about 230 K in the stratosphere), then $P_s < P_s^0$ and the particle will evaporate. This occurs at about 30-km altitude in the stratosphere and thus that altitude roughly defines the top of the stratospheric aerosol layer.

References

- Appenzeller, C., and H. C. Davies, 1992: Structure of stratospheric intrusions into the troposphere. *Nature*, **358**, 570–572.
- Brewer, A. M., 1949: Evidence for a world circulation provided by the measurements of helium and water vapor distribution in the stratosphere. *Quart. J. Roy. Meteor. Soc.*, **75**, 351–363.
- Brock, C. A., P. Hamill, J. C. Wilson, H. H. Jonsson, and K. R. Chan, 1995: Particle formation in the upper troposphere: A source of nuclei for the stratospheric aerosol. *Science*, **270**, 1650–1653.
- Chen, P., J. R. Holton, A. O'Neill, and R. Swinbank, 1994: Isentropic mass exchange between the Tropics and extratropics in the stratosphere. *J. Atmos. Sci.*, **51**, 3006–3018.
- Chin, M., and D. D. Davis, 1995: A reanalysis of carbonyl sulfide as a source of stratospheric background aerosol. *J. Geophys. Res.*, **100**, 8993–9005.
- Clarke, A. D., 1993: Atmospheric nuclei in the Pacific midtroposphere: Their nature, concentration and evolution. *J. Geophys. Res.*, **98**, 20 633–20 647.
- COESA, 1967: *U.S. Standard Atmosphere Supplements, 1966*. U.S. Government Printing Office, 289 pp.
- Dobson, G. M. B., 1956: Origin and distribution of polyatomic molecules in the atmosphere. *Proc. Roy. Soc. London Ser. A*, **236**, 187–193.
- Doyle, G. J., 1961: Self-nucleation in the sulfuric acid–water system. *J. Chem. Phys.*, **35**, 795–799.
- Fiocco, G., and G. Grams, 1964: Observations of the aerosol layer at 20 km by optical radar. *J. Atmos. Sci.*, **21**, 323–324.
- Fuchs, N. A., 1964: *The Mechanics of Aerosols*. Pergamon Press, 408 pp.
- Goodman, J., K. G. Snetsinger, G. V. Ferry, N. H. Farlow, H. Y. Lem, and D. M. Hayes, 1982: Altitude variations in stratospheric aerosols of a tropical region. *Geophys. Res. Lett.*, **9**, 609–612.
- Grant, W. B., E. V. Browell, C. S. Long, L. L. Stowe, R. G. Grainger, and A. Lambert, 1996: Use of volcanic aerosols to study the tropical stratospheric reservoir. *J. Geophys. Res.*, **101**, 3973–3988.
- Hamill, P., 1975: The time dependent growth of H₂O - H₂SO₄ aerosols by heteromolecular condensation. *J. Aerosol Sci.*, **6**, 475–482.
- , C. S. Kiang, and R. D. Cadle, 1977a: The nucleation of H₂SO₄ - H₂O solution aerosol particles in the stratosphere. *J. Atmos. Sci.*, **34**, 150–162.
- , O. B. Toon, and C. S. Kiang, 1977b: Microphysical processes affecting stratospheric aerosol particles. *J. Atmos. Sci.*, **34**, 1104–1119.
- , R. P. Turco, C. S. Kiang, O. B. Toon, and R. C. Whitten, 1982: An analysis of various nucleation mechanisms for sulfate particles in the stratosphere. *J. Aerosol Sci.*, **13**, 561–585.
- Hitchman, M. H., M. McKay, and C. R. Trepte, 1994: A climatology of stratospheric aerosol. *J. Geophys. Res.*, **99**, 20 689–20 700.
- Holton, J. R., P. H. Haynes, M. E. McIntyre, A. R. Douglass, R. R. Rood, and L. Pfister, 1995: Stratospheric–tropospheric exchange. *Rev. Geophys.*, **33**, 403–439.
- Hoskins, B. J., 1991: Toward a PV–Theta view of the general circulation. *Tellus*, **43(AB)**, 27–35.
- Jensen, E. J., O. B. Toon, H. B. Selkirk, J. D. Spinhirne, and M. R. Schoeberl, 1996: On the formation and persistence of subvisible cirrus clouds near the tropical tropopause. *J. Geophys. Res.*, **101**, 21 361.
- Junge, C. E., C. W. Chagnon, and J. E. Manson, 1961: Stratospheric aerosols. *J. Meteor.*, **18**, 81–108.
- Kiang, C. S., and D. Stauffer, 1973: Chemical nucleation theory for various humidities and pollutants. *Faraday Sym. Chem. Soc.*, **7**, 26–33.
- Loewenstein, M., J. R. Podolske, K. R. Chan, and S. E. Strahan, 1989: Nitrous oxide as a dynamical tracer in the 1987 airborne Antarctic ozone experiment. *J. Geophys. Res.*, **94**, 11 589–11 598.
- McCormick, M. P., P. Hamill, T. J. Pepin, W. P. Chu, T. J. Swissler, and L. R. McMaster, 1979: Satellite studies of the stratospheric aerosol. *Bull. Amer. Meteor. Soc.*, **60**, 1038–1046.
- , and Coauthors, 1981: High latitude stratospheric aerosols measured by the SAM II satellite system in 1978 and 1979. *Science*, **214**, 328–331.
- , H. M. Steele, P. Hamill, W. P. Chu, and T. J. Swissler, 1982: Polar stratospheric cloud sightings by SAM II. *J. Atmos. Sci.*, **39**, 1387–1397.
- , T. J. Swissler, W. H. Fuller, W. H. Hunt, and M. T. Osborne, 1984: Airborne and ground-based lidar measurements of the El Chichón stratospheric aerosol from 90°N to 56°S. *Geophys. Int.*, **23**, 187–221.
- , P. Wang, and L. Poole, 1993: Stratospheric aerosols and clouds. *Aerosol–Cloud–Climate Interactions*, P. V. Hobbs, Ed., Academic Press, 205–222.
- Pinnick, R. G., J. M. Rosen, and D. J. Hofmann, 1976: Stratospheric aerosol measurements III: Optical model calculations. *J. Atmos. Sci.*, **33**, 304–413.
- Pitari, G., V. Rizi, L. Ricciardulli, and G. Visconti, 1993: High-speed civil transport impact: The role of sulfate, nitric acid trihydrate and ice aerosols studied with a two-dimensional model including aerosol physics. *J. Geophys. Res.*, **98**, 23 141–23 164.
- Plumb, R. A., 1996: A “tropical pipe” model of stratospheric transport. *J. Geophys. Res.*, **101**, 3957–3972.
- Price, J. D., and G. Vaughan, 1993: The potential for stratosphere–troposphere exchange in cut-off-low systems. *Quart. J. Roy. Meteor. Soc.*, **119**, 343–365.
- Profitt, M. H., and Coauthors, 1989: A chemical definition of the boundary of the Antarctic ozone hole. *J. Geophys. Res.*, **94**, 11 437–11 448.
- Read, G. W., L. Froidevaux, and J. W. Waters, 1993: Microwave limb sounder measurements of stratospheric SO₂ from the Mt. Pinatubo volcano. *Geophys. Res. Lett.*, **20**, 1299–1302.
- Reiss, H., 1950: The kinetics of phase transitions in binary systems. *J. Chem. Phys.*, **18**, 840–848.

- Rosen, J. M., 1964: The vertical distribution of dust to 30 km. *J. Geophys. Res.*, **69**, 4673–4676.
- , 1971: The boiling point of stratospheric aerosols. *J. Appl. Meteor.*, **10**, 1044–1045.
- Rosenlof, K. H., 1995: The seasonal cycle of the residual mean meridional circulation in the stratosphere. *J. Geophys. Res.*, **100**, 5173–5191.
- , and J. R. Holton, 1993: Estimates of the stratospheric residual circulation using the downward control principle. *J. Geophys. Res.*, **98**, 10 465–10 479.
- Steele, H. M., and P. Hamill, 1981: Effects of temperature and humidity on the growth and optical properties of sulphuric acid–water droplets in the stratosphere. *J. Aerosol Sci.*, **12**, 517–528.
- Thomason, L. W., G. S. Kent, C. R. Trepte, and L. R. Poole, 1997: A comparison of the stratospheric aerosol background periods of 1979 and 1989–1991. *Geophys. Res. Lett.*, in press.
- Tie, X. X., X. Lin, and G. Brasseur, 1994: Two-dimensional coupled dynamical/chemical/microphysical simulation of global distribution of El Chichón volcanic aerosol. *J. Geophys. Res.*, **99**, 16 779–16 792.
- Toon, O. B., R. P. Turco, P. Hamill, C. S. Kiang, and R. C. Whitten, 1979: A one-dimensional model describing aerosol formation and evolution in the stratosphere: II. Sensitivity studies and comparison with observations. *J. Atmos. Sci.*, **36**, 718–736.
- Trepte, C. R., and M. Hitchman, 1992: Tropical stratospheric circulation deduced from satellite aerosol data. *Nature*, **355**, 626–628.
- , R. E. Veiga, and M. P. McCormick, 1993: The poleward dispersal of Mount Pinatubo volcanic aerosol. *J. Geophys. Res.*, **98**, 18 563–18 575.
- Turco, R. P., P. Hamill, O. B. Toon, R. C. Whitten, and C. S. Kiang, 1979: A one-dimensional model describing aerosol formation and evolution in the stratosphere: I. Physical processes and mathematical analogs. *J. Atmos. Sci.*, **36**, 699–717.
- Young, R., H. Houben, and O. B. Toon, 1994: Radiatively forced dispersion of the Mt. Pinatubo volcanic cloud and induced temperature perturbations in the stratosphere during the first few months following the eruption. *Geophys. Res. Lett.*, **21**, 369–372.
- Yue, G. K., and A. Deepak, 1984: Latitudinal and altitudinal variation of size distribution of stratospheric aerosols inferred from SAGE aerosol extinction coefficient measurements at two wavelengths. *Geophys. Res. Lett.*, **11**, 999–1002.
- , M. P. McCormick, and E. W. Chiou, 1991: Stratospheric aerosol optical depth observed by the stratospheric aerosol and gas experiment II: Decay of the El Chichón and Ruiz volcanic perturbations. *J. Geophys. Res.*, **96**, 5209–5219.
- Zhao, J., O. B. Toon, and R. P. Turco, 1995a: Origin of condensation nuclei in the springtime polar stratosphere. *J. Geophys. Res.*, **100**, 5215–5227.
- , R. P. Turco, and O. B. Toon, 1995b: A model simulation of Pinatubo volcanic aerosols in the stratosphere. *J. Geophys. Res.*, **100**, 7315–7328.